

Land Use/Cover Change and Its Policy Implications in Typical Agriculture-forest Ecotone of Central Jilin Province, China

DONG Yulin^{1,2}, REN Zhibin¹, FU Yao³, YANG Ran⁴, SUN Hongchao^{1,2}, HE Xingyuan^{1,2}

(1. Key Laboratory of Wetland Ecology and Environment, Northeast Institute of Geography and Agroecology, Chinese Academy of Sciences, Changchun 130102, China; 2. University of Chinese Academy of Sciences, Beijing 100049, China; 3. School of Geography and Engineering of Land Resources, Yuxi Normal University, Yuxi 653100, China; 4. College of Earth Sciences, Jilin University, Changchun 130012, China)

Abstract: During the 21st century, policies toward agriculture, forestry, and urbanization have emerged to ensure food security, ecological restoration, and human well-being by managing land in Northeast China. However, the integrated effects and relationships of various policies are still not well understood. This study observed the land use land cover changes in Central Jilin from 2000 to 2019 and, by considering policy involvement, aimed to understand the effects and trade-offs of policies. Results showed that the cropland, including dryland and rice paddy, and the forest, including coniferous forest and deciduous forest, are dominant land types in Central Jilin. During 2000–2019, the land changed diversely, of which the main changes were the expanded dryland (+0.43 million ha), the increased deciduous forest (+22 million ha), the decreased coniferous forest (−0.08 million ha), and the expanded urban settlement (+0.04 million ha). With these changes, despite the unit grain yield showing a rising trend, the yield contribution of Central Jilin to the national total decreased. The poor cultivating structure made for the cropland expansion and reduced the implementation space of environmental restoration projects such as the Grain to Green. Thus, in Central Jilin that transits from the agri-food production zone to the eco-regulation zone, environmental projects coexisted in a trade-off manner with agricultural policies that aim to liberate agricultural productivity. In the key urban agglomerations of Central Jilin, the increase in the proportion of green space improved the thermal environment and carbon balance. The gross domestic product of the large city and its local proportion also rose. These improvements benefited from the promotion of development policies and urbanization policies at key time points. In the future, it is necessary to coordinate agricultural policies and environmental projects and promote the progress of small- and medium-sized cities to ensure the equality of regional development. This study has implications for making decisions to revitalize Northeast China and researchers who inform decisions.

Keywords: land use land cover (LULC); policy; agriculture-forest ecotone; urbanization; Northeast China

Citation: DONG Yulin, REN Zhibin, FU Yao, YANG Ran, SUN Hongchao, HE Xingyuan, 2021. Land Use/Cover Change and Its Policy Implications in Typical Agriculture-forest Ecotone of Central Jilin Province, China. *Chinese Geographical Science*, 31(2): 261–275. https://doi.org/10.1007/s11769-021-1189-5

1 Introduction

Ecotone, the transition area between two dominant eco-

systems, is rich in ecological functions and biological flows but very sensitive to human activities (Ye and Fang, 2012). Because both agricultural production and

Received date: 2020-08-20; accepted date: 2020-12-17

Foundation item: Under the auspices of Science and Technology Major Project of Jilin Province (No. 20200503001SF), Youth Innovation Promotion Association of Chinese Academy of Sciences (No. 2020237), Cooperative Project of Jilin Province and Chinese Academy of Sciences for Industrializing Advanced Technology (No. 2020SYHZ0004), National Natural Science Foundation of China (No. 41701210)

Corresponding author: HE Xingyuan. E-mail: hexingyuan@iga.ac.cn

© Science Press, Northeast Institute of Geography and Agroecology, CAS and Springer-Verlag GmbH Germany, part of Springer Nature 2021

ecological conservation are critical to national security and local sustainability, the land change of agriculture-forest ecotone affects food supply, climate regulation, water yield, *etc.*, and thus human life. However, little attention on the agriculture-forest ecotone has been studied, especially for countries where the land system underwent rapid alteration, such as China. Policies are the primary driving factors of land change (Bryan et al., 2018; Kuang, 2020a); however, it is undetermined that policies realized various objectives, e.g., promoting food production while preserving environments, in the ecotone.

Land use land cover (LULC) changes, with the deep relationship to administrative measures, are affecting the biogeochemical process, wildlife habitats, energy exchange, and thereby on climate change, biodiversity, and public health (Lammert and Allan, 1999; Feddema et al., 2005; Liang et al., 2010; Houghton et al., 2012). The wealthy society could invest huge funds to reforest the poor land, preventing floods and sandstorms (Bryan et al., 2018). However, improper interventions could cause financial loss, biodiversity loss, and biomass loss (Liu et al., 2014; Lai et al., 2016; Ren et al., 2019). Agriculture ecosystem is the most important source to maintain human life, which encroached primary ecosystems and formed transitions from cropland to forest, grass, water, *etc.* (Ye and Fang, 2012; Liu et al., 2017; Wu et al., 2019). Previous studies indicated that proper land management could boost agricultural economy (Wu et al., 2019). However, cropland expansion stressed climate change in local agriculture-forest ecotone (Liu et al., 2017). To maintain the ecotone in a safe operating space (Rockstrom et al., 2009), assessing LULC changes is critical.

On the road of land exploitation-economic progress-ecological restoration, China's LULC changes affected by administrative measures in decades. For example, forests were exploited for supplying food and energy before 1978; hereafter, the central government invested huge funds for land management to restore land systems (Liu et al., 2008; Bryan et al., 2018). However, the pace of Northeast China is different. The economic downturn and poor industrial structure made the land use in Northeast China unbalanced, e.g., the proportion of cropland has exceeded 1/3 (Mao et al., 2019). On the other hand, dual tasks of national importance, i.e., food production and ecological restoration, guide the land

management in Northeast China; thus, LULC changes, represented by cropland expansion and forest restoration, were complicated (Chen et al., 2015). In the 21st century, a series of administrative measures were unveiled by the central government for ensuring economy recovery, grain production and ecological restoration, which collectively drove LULC changes in Northeast China. For example, when the Grain to Green project was fully implemented in 2003, the forest area increased (Zhao et al., 2019b). In 2009 with the national plan of securing food supply announced, cropland expanded for more yield (Mao et al., 2018).

The coexistence of various policies potentially forms trade-off relationships. Previous studies indicated that agriculture and forestry policies constituted trade-offs; agriculture policies encouraged cropland expansion that exacerbated forest clearing, hindering ecological restoration (Lai et al., 2016). Under economic development goals, disordered urban expansion encroached on cropland, weakened grain production (He et al., 2017). With the implementation of various policies and projects, the agriculture-forest ecotone of Northeast China, central Jilin Province (JLC), is suitable for looking back at LULC changes and policy interrelationships. The measures include environmental projects such as the Grain to Green; the development strategy such as the Northeast China Revitalization; and agricultural policies such as abolishing agricultural taxes; the total number of twelve measures is outstanding in Northeast China (Mao et al., 2019). However, it is undetermined these policies were synergistically achieving their respective goals by driving LULC changes. As a result, decision-makers cannot properly adjust policies and projects that originally served to revitalize Northeast China and achieve sustainable development.

To assist the government and corporations in making decisions on policy and investment, as well as researchers who inform these decisions, we aim to explore the LULC changes and policy evolution in JLC. The present study developed a 15 m resolution LULC dataset with a 5-year interval from 2000 to 2019. The LULC dataset, combined with socio-economic statistics, matches the time nodes of various policies, which could be used to learn the influence of various policies on both land and socio-economy. We answered two key questions: 1) how the LULC changed and its effects in JLC during 2000–2019, and 2) whether policies, through affecting

LULC change, formed trade-off interrelationships. To revitalize Northeast China and ensure regional progress equality, this study proposed policy options and land use issues that need attention.

2 Material and Methods

2.1 Study area

An agriculture-forest ecotone in central Jilin Province (JLC), Northeast China, was selected for this study (Fig. 1). JLC consists of four cities, including Changchun, Jilin, Siping and Liaoyuan, with an area extent about 10.9×10^6 ha and a population about 16.0×10^6 . JLC has comprehensive LULC types include forest, cropland, water, bare ground, built-up area (Zhao et al., 2019b; Dong et al., 2020a); diverse landforms with an elevation of 103–1399 m; and the temperate continental climate. As an agriculture-forest ecotone, JLC was risked by long-term human activities, resulted in habitat degradation, water loss, and sandstorms (Kuang and Yan, 2018; Mao et al., 2019). During the 21st century, JLC underwent various administrative measures of agriculture, forestry, and urbanization. The projects of Grain to Green, Three-North Shelter Forest, and Natural Forest Conservation aim to plant more forest in poor

lands. According to the National Eco-Function Zoning Plan (MEE, 2015), approximately two-third area of JLC is the agricultural food production zone. JLC also includes an ecological regulation zone that aims to restore the environment through environmental projects. Besides, Changchun City and Jilin City integrated into a key urban agglomeration that is located on the cross of the Belt and Road.

2.2 Data and preprocessing

By using Calibrated Top of Atmosphere Reflectance (TOA) images, which were captured by Landsat instruments Enhanced Thematic Mapper Plus (ETM+) and Operational Land Imager (OLI), LULC data of the present study were generated in Google Earth Engine (GEE). For each year, approximately 150 images of path 117–119 and row 29–30 were used. Based on phenological difference, the vegetation land types such as coniferous forests and deciduous forests were mapped. Thus, the fluctuation of the vegetation index during the year was used to filter the images (Dong et al., 2020b). Within a mapping period, such as the growing season, all TOA images with cloud-likelihood of less than 25 were used and reduced into one image by median stacking for mapping LULC. Furthermore, the

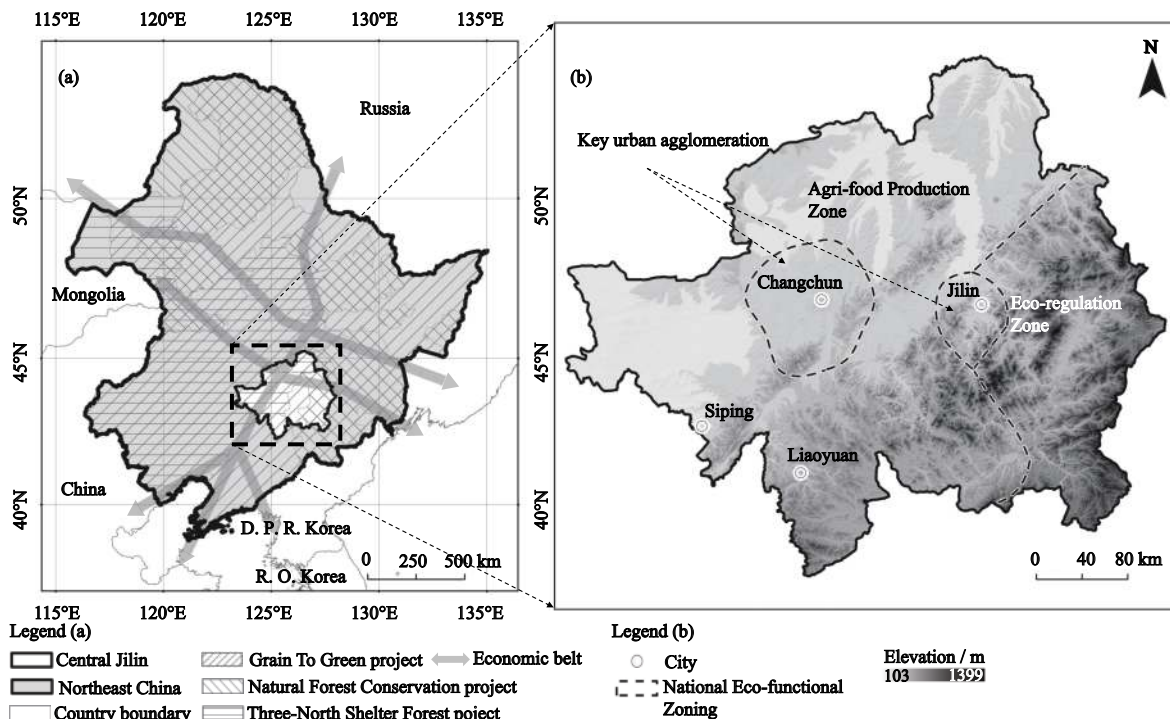


Fig. 1 The geographic location of central Jilin Province (JLC) and spatial extent of part administrative measures

spatial resolution of TOA images was enhanced to 15 m through a sliding-window algorithm that built on the GEE environment (Dong et al., 2020a). Through this approach, original spectral information of TOA images was saved and thus served for constructing finer resolution spectral indices include Normalized Difference Vegetation Index (*NDVI*) and Modified Normalized Difference Water Index (*MNDWI*) (Dong et al., 2016; Yang et al., 2020).

$$NDVI = (B_{nir} - B_{red}) / (B_{nir} + B_{red}) \quad (1)$$

$$MNDWI = (B_{green} - B_{swir1}) / (B_{green} + B_{swir1}) \quad (2)$$

where B_{green} , B_{red} , B_{nir} , and B_{swir1} denote spectral reflectance measurements acquired in the green, red, near-infrared, and shortwave infrared-1 bands, respectively. Also, the shortwave infrared-2 band (*SWIR2*) and thermal infrared-1 band (*TIR1*) were applied to map settlements and eliminate building shadows, respectively. The *NDVI* was applied to simulate phenology (Dong et al., 2020a). For reducing the saturation effect of *NDVI*, the index Fraction of Vegetation Cover (*FVC*) was constructed to extract vegetation (Yang et al., 2020).

$$FVC = (NDVI - NDVI_{soil}) / (NDVI_{veg} - NDVI_{soil}) \quad (3)$$

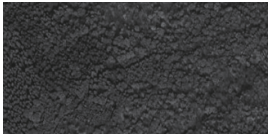
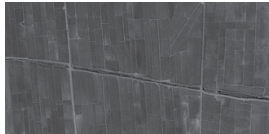

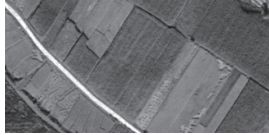

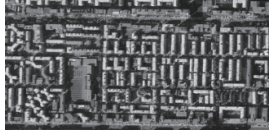
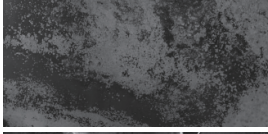

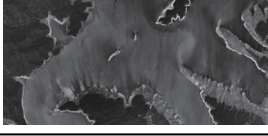
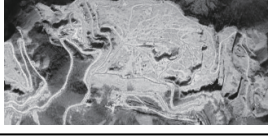
where $NDVI_{veg}$ and $NDVI_{soil}$ were quantified from the *NDVI* histogram; $NDVI_{soil}$ is the average of 0–0.5% value segment; $NDVI_{veg}$ is the average of 99.5%–100.0% value segment.

The VIIRS nightlight images (VIIRS NT) were applied to extract the urbanized area. The product MOD11A1.006 was employed to simulate land surface temperature (LST) (Dong et al., 2016); its bad pixels were masked by the 8-bit quality band. The product MOD17A3HGF was employed to simulate net primary production (NPP). The product Global Annual PM_{2.5} Grids was applied to simulate Fine Particulate Matter (PM_{2.5}) during 2000–2016 in urbanized areas (van Donkelaar et al., 2016). Besides, the annual record of crop yield was collected from Statistic Yearbooks of Jilin Province (downloaded via <http://tjj.jl.gov.cn/>).

2.3 Mapping land use land cover by Multilevel Decision Rule classifier

Considering the environmental background and mapping capacity, we defined a LULC category of the forest, grassland, wetland, water body, cropland, impervious, and bareland (Table 1). The shrub was integrated

Table 1 Land use land cover category and image examples from Google Earth in Central Jilin Province, China

LULC category		Google Earth example	LULC category		Google Earth example
Tier1	Tier2		Tier1	Tier2	
Forest	Coniferous forest		Cropland	Rice paddy	
	Deciduous forest			Dryland	
Grass			Impervious	Urban settlement	
Wetland				Rural settlement	
			Bareland		
Water					

into the forest category because the plant structure cannot be specifically defined. Instead, the forest category was classified as coniferous forest and deciduous forest by simulating phenology. The cropland category was further classified as rice paddy and dryland. The impervious category was further classified as urban settlement and rural settlement.

The Multilevel Decision Rule (MDR), a JavaScript-based LULC classifier, was used in this study (Dong et al., 2020a). The MDR is an automatic process that can extract LULC orderly through thresholding spectral indices or bands. As the component of the MDR, each decision rule segments an image into two classes of pixels (Dong et al., 2020b). For example, within an *NDVI* image, setting pixel values of less than 0.01 as the water; and regarding others as the non-water area (Mao et al., 2018). To determine thresholds, the OTSU algorithm was employed (Otsu, 1979).

The indicator day of year (DOY) was applied to guide median stacking that constructs a single image that represents a period of interest; thereby, mapping target LULC according to phenology. For example, vegetation extent was classified by a single *FVC* image that represents the median value during DOY of 180–250 (Fig. 2). The forest extent was mapped based on median *NDVI* during DOY of 120–170 when the daytime accumulated temperature less than the standard of 1900°C for crops growing. The extents of coniferous forest and

deciduous forest were identified based on median *NDVI* of the withering period, i.e., DOY of 25–75 and 300–325. For grassland mapping, we applied median *SWIR2* to extract grass. In cropland extents, the rice paddy was mapped by using median *MNDWI* during the start of the transplanting period (Dong et al., 2016).

The non-vegetation area includes impervious, water, and wetland. The preliminary impervious extent was mapped by the shortwave band; the *SWIR2* was used because of fewer dispersions compared with *SWIR1*. By using VIIRS NT (nighttime light) data, the impervious was classified as urban settlements and rural settlements. Because the water area is dynamic in a year, we firstly mapped the water surface area of big reservoirs during the year. Results showed that images from April, May, September, and October could be used to obtain the maximum extent of water; thereby, we mapped water extent by median *MNDWI* of these four months. Hereafter, we mapped the wetland, defined as flooded vegetation, by setting the Boolean rule of median *MNDWI* less than median *NDVI*. Furthermore, we removed shadows from water by adjusting *TIR1* (Dong et al., 2020a).

2.4 Accuracy assessment

The accuracy was assessed by a statistically robust method, based on the sample count matrix and the areal weight of LULC (Olofsson et al., 2014). We applied a

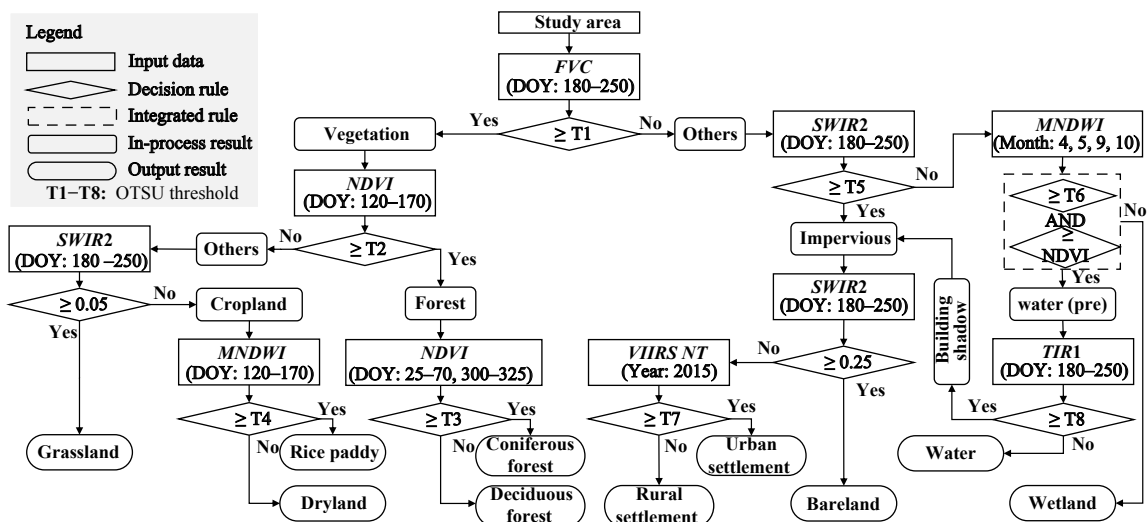


Fig. 2 The flow chart shows the sequence of land use land cover mapping. The filtration of images was according to phenology and properly adjusted DOY to ensure the image quality. FVC: fraction of vegetation cover; SWIR2: shortwave infrared-2 band; NDVI: normalized difference vegetation index; MNDWI: modified normalized difference water index; TIR1: thermal infrared-1 band; VIIRS NT: nighttime light; DOY: day of year. T1–T8 are thresholds that segment an image into two types of pixels

published sample set collected from high-resolution satellite images of 2016 and 2017 for assessing our 2015 LULC map (Zhao et al., 2019a). The set includes 258 cropland samples, 395 forest samples that did not be classified as coniferous forest or deciduous forest, 115 grassland samples, 384 impervious samples, and 354 water samples. The set also contains 238 forest samples from the withering season of 2016, which were used to assess the accuracy of mapping result coniferous forest. Furthermore, we randomly collected 216 deciduous forest samples, 204 rice paddy samples, 256 dryland samples, 100 wetland samples, and 153 bareland samples from 2014–2016 images of Google Earth. Because definite samples of urban settlement and rural settlement cannot be collected, we tested the accuracy of mapping result impervious. The result reported that the overall accuracy of our LULC data reached 0.939 ± 0.016 (Table S1). Especially, tier-2 LULC types, including coniferous forest, deciduous forest, rice paddy, and dryland, showed high user's accuracy ($\geq 0.910 \pm 0.03$) and producer's accuracy ($\geq 0.875 \pm 0.04$), laid a good foundation for observing LULC changes.

2.5 Analysis of land use land cover change

Changes in land cover were directly computed in the software ArcGIS 10.2. The forest and grassland were merged as green space to observe urban land changes (Ren et al., 2019; Kuang, 2020c; Kuang and Dou, 2020). To track the spatial trajectory of urban land use, the patch density (PD) was computed by using the software Fragstats 4.2; the centroids of land patches were obtained by using the software ArcGIS 10.2. Furthermore, we computed the crop yield based on LULC data.

$$Y_{i,k} = TY_{i,k}/A_{i,k} \quad (4)$$

where $Y_{i,k}$ denotes the yield per hectare of the crop type i in year k . The $TY_{i,k}$ denotes the total yield. The $A_{i,k}$ denotes the area of dryland or rice paddy from our maps. This study analyzed two types of crops includes major crops (of dryland) and rice paddy to coordinate with the land category of dryland and rice paddy. The major crop type is the total of maize and soybean. The cost and profit information of crop cultivation was collected from the National Agricultural Product Cost-Benefit Collection (<https://www.yearbookchina.com/>).

3 Results

3.1 LULC change and its effect on agriculture production

The cropland was the most covered LULC type in JLC (Fig. 3). During 2000–2019, the dryland area increased from 4.87×10^6 ha to 5.31×10^6 ha; the rice paddy area slightly changed around 0.65×10^6 ha after the expansion in 2000–2005. The forest was widely distributed in the east JLC. During 2000–2019, the coniferous forest area slightly decreased from 1.57×10^6 ha to 1.49×10^6 ha; however, the deciduous forest area increased significantly from 1.05×10^6 ha to 1.28×10^6 ha. During 2000–2005, the urban settlement area was unchanged as 0.07×10^6 ha; after 2005, the urban settlement expanded to 0.11×10^6 ha in 2019. By contrast, the rural settlement area lost significantly from 0.88×10^6 ha to 0.22×10^6 ha during 2000–2019, especially in the west JLC (Fig. 3). Among other land covers, the area of water body fluctuated between 0.13×10^6 ha and 0.14×10^6 ha; the wetland area decreased from 0.05×10^6 ha to 0.02×10^6 ha; the grassland area increased to 0.01×10^6 ha. The change of bareland area showed a v-trend as decreased in 2000–2010 and increased in 2010–2019, resulted in 0.13×10^6 ha in 2019.

Although the cropland area increased continually, the importance of the agricultural economy decreased. The contribution of the agricultural sector to total GDP decreased from 9.2% to 3.5% (Fig. 4b). The increment of major crops yield was similar to the dryland expansion, from 2.0×10^3 kg/ha to 3.5×10^3 kg/ha (Fig. 4f). However, with the agricultural GDP proportion decreased, the major crop yield decreased from 2015 to 2019. The rice yield increased slightly from 4.3×10^3 kg/ha to 4.6×10^3 kg/ha; whereas compared with the continuous increment in national yield, that of JLC was discrepant (Fig. 4e). What is more, after 2005, the yield proportion of JLC to the national total decreased by 0.61% and 0.2% in major crops and rice, respectively (Fig. 4d). The situation likely related to the Grain to Green project that was fully implemented in 2003 because the net area of cropland to forest had reduced since the period 2005–2010 (Fig. 4a). Moreover, the proportion of rural population decreased after 2005 (Fig. 4c), indicating the decoupling of grain yield and rural human power. In general, despite the cropland area increased continually, the agriculture development of JLC was lagging to the

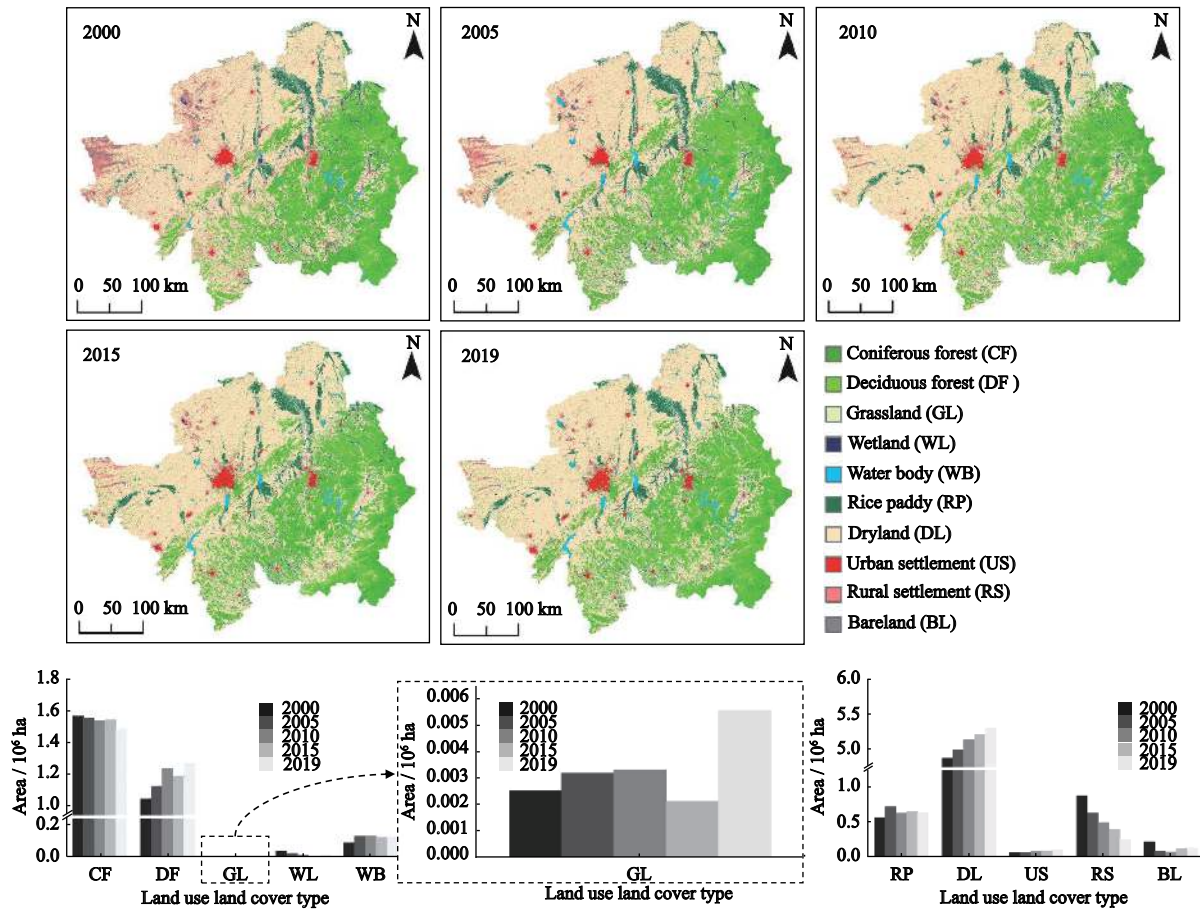


Fig. 3 Spatiotemporal changes in land use land cover (LULC) of JLC during 2000–2019

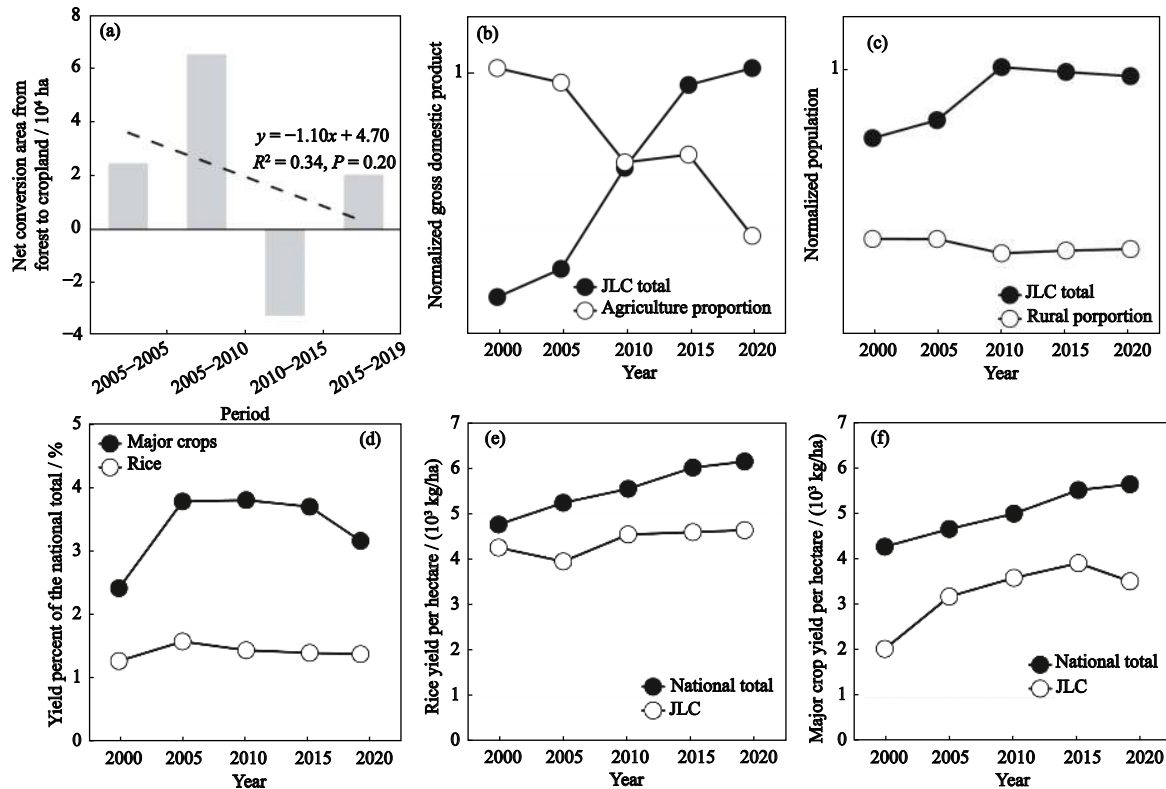


Fig. 4 The change of agriculture-related factors of JLC in 2000–2019. The type of major crops includes maize and soybean

national development.

3.2 LULC change and its effect on urban environment

In the key urban agglomeration, the expansion of green space and urban settlement was observed (Fig. 5). During 2000–2019, urban settlement expanded approximately 17.2×10^3 ha in Changchun and 2.7×10^3 ha in Jilin, respectively. The expansion was obvious after 2005; however, the expansion direction was different in cities, i.e., northeastward in Changchun while northwestward in Jilin (Fig. 6). Besides, during the period considered, the area of green space increased from 1.0×10^3 ha to 7.3×10^3 ha in Changchun City and from 0.3×10^3 ha to 1.4×10^3 ha in Jilin City. In both cities, the increment of green space could be divided into two-phase including 2000–2010 and 2010–2019. Although the total area of green space was distinct in the two cit-

ies, the proportion was similar, i.e., increased from 1.4% to 10.2% in Changchun City and from 1.4% to 7.3% in Jilin City.

The spatial trajectory of settlement and green space was divided into two phases by the year 2010. The PD of green space increased dramatically in 2000–2010 while kept slightly changing in 2010–2019 (Fig. 6a), indicating urban greening turned from rapid to slow. By contrast, the PD of settlement turned from decreasing to increasing in 2010 (Fig. 6b), indicating urban sprawl boosted after 2010. Nonetheless, the settlement and green space were sprawled in similar directions (Fig. 6). This spatial trajectory of gray space and green space mitigated the urban thermal environment and air pollution.

The settlement expansion that generated paved areas could increase the LST and air pollution in the outer city. The history centroid of maximum LST and $PM_{2.5}$

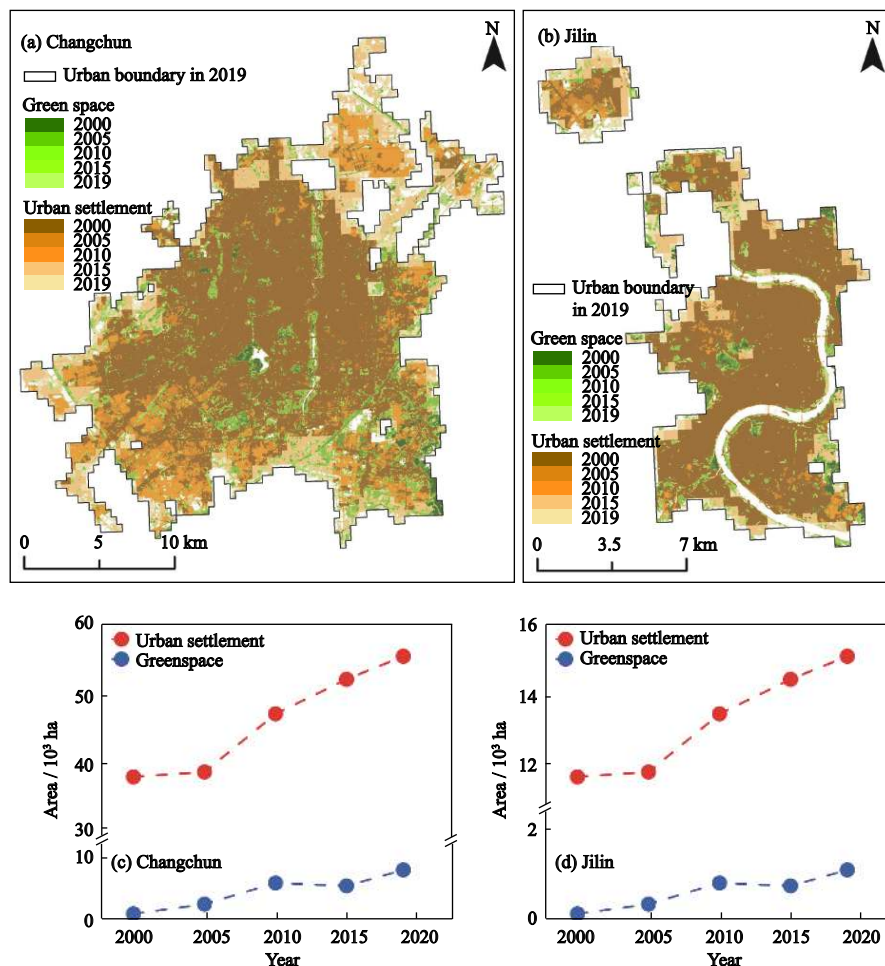


Fig. 5 Spatiotemporal changes in urban settlement and green space in Changchun and Jilin cities of Central Jilin Province, China

approximately shifted along with the direction of settlement expansion, i.e., northwestward in Changchun City and northeastward in Jilin City (Fig. 6). During 2000–2015, the shift of $PM_{2.5}$ centroid matched with settlement centroid; and the average $PM_{2.5}$ increased significantly from $23.89 \mu\text{g}/\text{m}^3$ to $70.02 \mu\text{g}/\text{m}^3$ in Changchun City and from $25.91 \mu\text{g}/\text{m}^3$ to $60.22 \mu\text{g}/\text{m}^3$ in Jilin City (Fig. 6e). Nevertheless, the maximum LST and NPP obtained mitigation. During the period considered, the urban NPP increased from $247 \text{ g C}/(\text{m}^2\cdot\text{yr})$ to $349 \text{ g C}/(\text{m}^2\cdot\text{yr})$ in Changchun City and from $308 \text{ g C}/(\text{m}^2\cdot\text{yr})$ to $441 \text{ g C}/(\text{m}^2\cdot\text{yr})$ in Jilin City (Fig. 6d); the maximum LST decreased from 48°C to 42°C in

Changchun City and from 46°C to 41°C in Jilin City, respectively (Fig. 6c). These changes, coupled with the increment of the green space (Fig. 5), suggest the important role of urban green space in carbon balance and thermal mitigation. Before 2010, the green space area increased rapidly but of gradual fragmentation (Fig. 6a), which merely generated a short improvement of LST and NPP (Fig. 6c, Fig. 6d). By comparison, after 2010, the PD of green space increased mildly in Changchun City and temporarily decreased in Jilin City, which, however, formed robust biomass to sustain improvement of thermal environment and carbon balance. In this regard, to enhance the urban environment through urb-

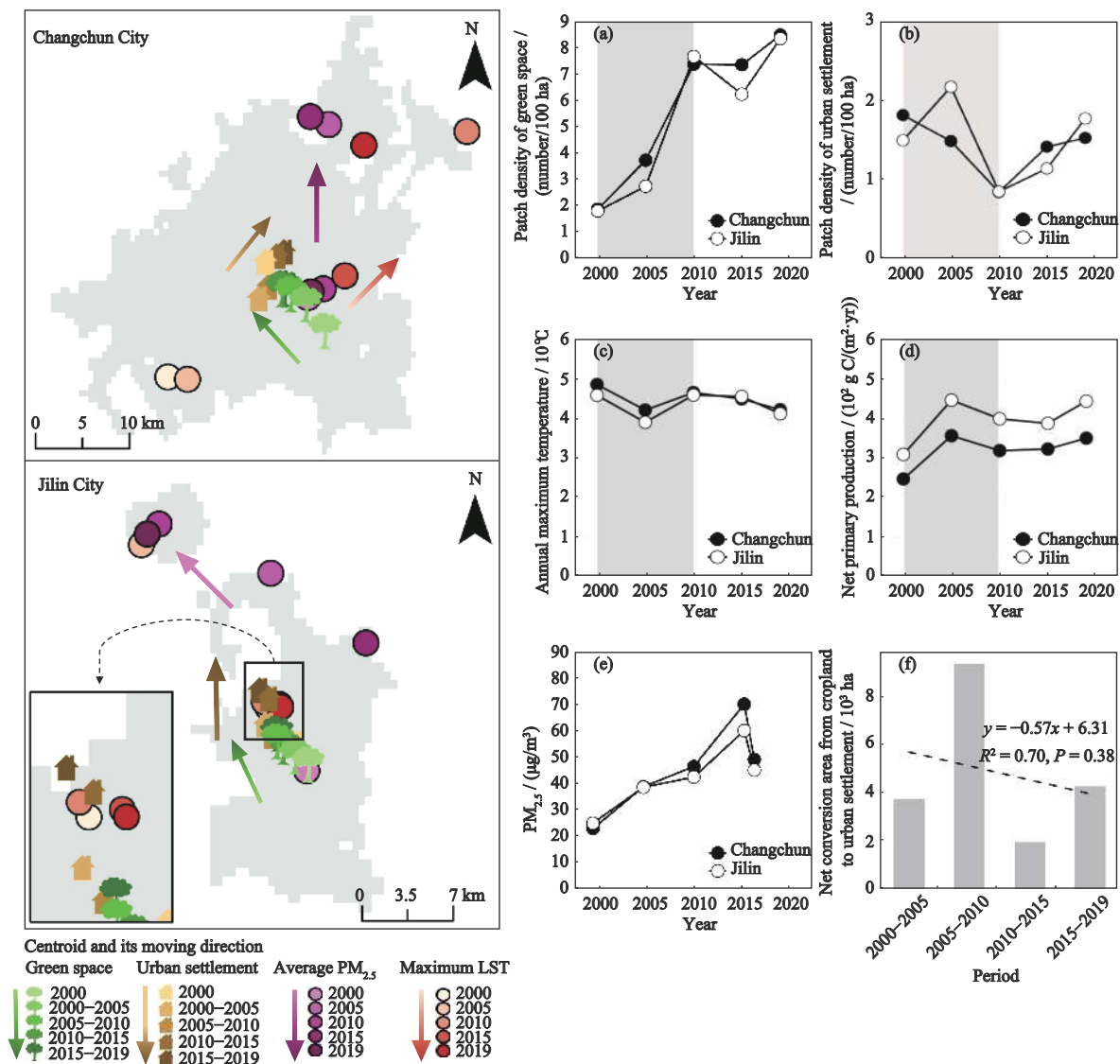


Fig. 6 Spatiotemporal changes in urban settlement, green space, and environmental factors in the Changchun-Jilin urban agglomeration. The gray bands on panels (a, b, c, d) indicate different trends of data changes. LST is land surface temperature

an greening, more attention should be paid to spatial configuration rather than merely areal increment.

4 Discussion

4.1 Policy related trade-offs between agricultural development and environmental restoration

Northeast China, with fertile soils and flat landforms, is suitable for agricultural development; thereby, its natural ecosystems have altered to cropland for securing the national staple food supply (Chen et al., 2015; Luo et al., 2018; Mao et al., 2019). As the transition from the agriculture supply zone to the ecological conservation zone (MEE, 2015), JLC is an important component of food production and environmental restoration in Northeast China. This study observed the decoupling of cropland expansion and agricultural development in JLC (Fig. 3, Fig. 4). Since policies are the primary driver of the LULC change and have been shifting to environmental conservation in China (Kuang, 2020b), it is necessary to ensure the cropland change would not impact restoration projects.

During the 21st century, twelve administrative measures covered JLC (Table 2), revolved around the Northeast China Revitalization that aimed to recover the eco-

nomy, agriculture, and environment. Two policies, including the Agriculture Tax Abolition and the National Eco-Function Zoning Plan, liberated agricultural productivity and ensured that food supply is the major task of JLC. Echoing these policies, during 2000–2010, both cropland area and yield increased (Fig. 3, Fig. 4). The net area that transformed from forest to cropland has also increased by approximately 160% in 2005–2010 compared with that of 2000–2005 (Fig. 4a), even under the project Grain to Green, i.e., returning cropland into forests. After 2010, due to national policies, including the Three-North Shelter Forest and the Commercial Logging Prohibition, shifted to environmental restoration, cropland immediately net converted to the forest (Fig. 4a); thereby, the yield began to descent and indicated that grain production is sensitive to administrative measures. What is more, after 2015, the major crop yield ratio of JLC to national total decreased by 0.53% (Fig. 4d), despite the national total yield increased by 2.26% (Fig. 4f); in other words, the JLC's functionality of food supply weakened. Therefore, in JLC, environmental projects and agricultural policies that try to increase grain production form a certain trade-off relation; to achieve environmental restoration, it is necessary to control the cropland area to a certain extent.

Table 2 The brief introduction of administrative measures that cover JLC during 2000–2019.

Year	Measure	Attribute	Reference
2001	Joined the World Trade Organization	Economic	(PHRC, 2009)
2003	Drafted the Northeast China Revitalization	Economic, Environmental, Agricultural	(PHRC, 2009)
2003	Fully implemented the Grain to Green project*	Environmental	(CSC, 2002)
2005	Abolished the agriculture tax	Agricultural	(PHRC, 2009)
2008	Announced the National Eco-Functional Zoning Plan	Economic, Agricultural, Urbanization	(MEE, 2015)
2009	Affirmed the strategy of Northeast China Revitalization	Economic, Environmental, Agricultural	(CSC, 2009)
2011	Implemented the Targeted Poverty Alleviation project	Economic, Agricultural	(CCCPC, 2011)
2011	Implemented the 5th batch of Three-North Shelter Forest project	Environmental	(NFGA, 2013)
2013	Announced the Belt and Road Initiative	Economic	(Mao et al., 2019)
2014	Prohibition of commercial logging	Environmental	(Mao et al., 2019)
2014	Initialized the National New-Type Urbanization Plan	Urbanization, Agricultural	(CCCPC, 2014)
2016	Invested the Northeast China Revitalization	Economic, Environmental, Agricultural	(NDRC, 2016)

Notes: *The pilot project of the Grain to Green started in 1999, excluding Northeast China; it was officially executed nationwide in 2003

Since the farmer's income relies on grain cultivation, agricultural development is deeply related to poverty alleviation. In JLC, although GDP increased with the announcement of the Northeast China Revitalization strategy in 2005, the agriculture contribution dived sharply by 5.8% during 2000–2019 (Fig. 4b). As the major purpose of the strategy is to recover industry, the share of the agricultural GDP inevitably decreased, despite agricultural GDP increased during 2000–2015 (Fig. 7c). Nevertheless, farmers might not receive more benefits because the crop cultivating structure in JLC was poor. In the past two decades, the proportion of maize planting increased significantly by about 30%; and it remained above 80% during 2015–2019 (Fig. 7a). In contrast, the proportion of rice cultivation was relat-

ively stable at around 12%–14%, while the proportion of soybean cultivation declined by about 12%. These changes probably were because maize (523 CNY/ha) (CNY is Chinese yuan, yuan (RMB)) generated higher cash profits than soybean (265 CNY/ha) (Fig. 7b), and the water shortage limited the expansion of rice cultivating. However, cultivating maize also generated fewer profits because its cost-profit ratio was -12%/ha (Fig. 7d). As a result, a potential causal cycle of 'poor cultivating structure-low cash-profit-cropland expansion' was formed in JLC. Due to the decoupling between grain yield and rural human resources (Fig. 4), the policy could majorly stimulate agricultural development. The path to further promote agricultural development should be to optimize the local cultivating structure rather than

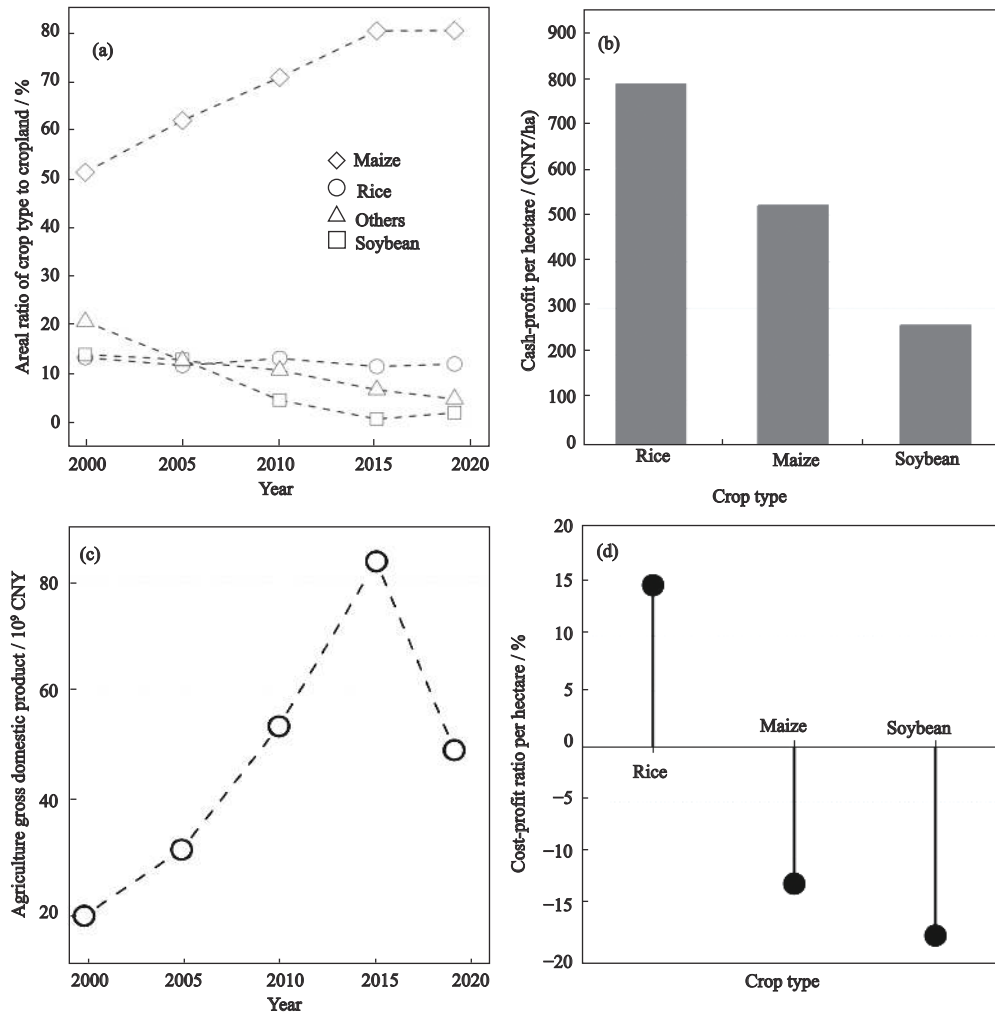


Fig. 7 The change of areal ratio and profit of crop types. (a) Change of areal ratio in crop types. (b) Cash-profit per hectare of major crop in 2015. (c) Change of agriculture GDP in JLC. (d) Cost-profit ratio per hectare of major crop types in 2015. CNY: Chinese yuan, equivalent to yuan (RMB)

to expand cropland. The Grain to Green project, in this way, could have more room for operation and thus boost the pace to restore the environment. Besides, an appropriate increase in the subsidy of forestry projects is an option for strengthening the momentum of environmental restoration.

4.2 Policy-driven LULC changes improved urban environment

The key urban agglomeration gathers most of the residents and economic output of JLC (Fig. 8d, Fig. 8e); however, the urban environment needs to be improved (Mao et al., 2019). By our observation, policies exerted a positive influence on the urban environment through driving LULC change, e.g., improved thermal environment and carbon balance (Fig. 6c, Fig. 6d), which is also reported by previous studies (Ren et al., 2018; Ren et al., 2019; Dong et al., 2020a). Policies promoted these improvements at key nodes, e.g., the Northeast China Revitalization drove the first ascent of green space ratio during 2000–2010 (Fig. 8c). After 2010, the National New-Type Urbanization Plan that asked for mitigating pollution and achieving urban sustainability drove the second ascent of green space ratio (Fig. 8c), which made for reducing LST and PM_{2.5} as well as increasing NPP (Fig. 6). Under that China's cities have been filled by impervious during the 21st century,

Changchun is representative in synergizing urban expansion and environmental improvement (Kuang, 2020b; Kuang and Dou, 2020), which manifested China's development vision of 'ecological civilization'.

Policies also boosted the economic progress in the urban agglomeration, which, with greening urban, shows the harmony of humans and land. For instance, in Changchun, GDP increased with the two rapid ascents of 2000–2015 and 2015–2019 (Fig. 8a). In this regard, at key time nodes, policies pushed these ascents. The first ascent was driven by joining the World Trade Organization and formulating the Northeast China Revitalization (Fig. 8a). Nonetheless, with the decrement of GDP proportion and population proportion in Changchun, the importance of the key city weakened. The affirmation of the Northeast China Revitalization strategy in 2009 rescued the absorption effect and the growth momentum of economy and population in the regional key city, Changchun (Fig. 8a, Fig. 8d). The Belt and Road Initiative, the National New-Type Urbanization Plan, and the investment of Northeast China Revitalization extended the economic progress and population boom after 2010 in Changchun (Fig. 8d, Fig. 8e). It is noted that both the GDP proportion and population proportion of Jilin showed a downward trend (Fig. 8d, Fig. 8e), which resulted from a strengthened absorption effect of the regional center city. Future policies need to

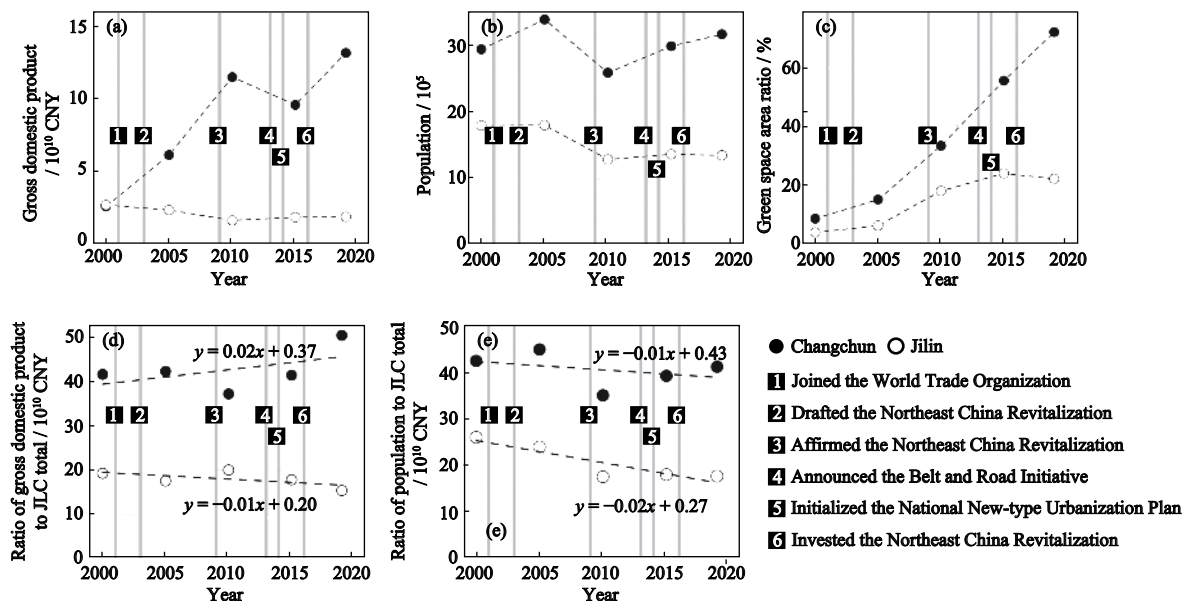


Fig. 8 The change of economy, population, and green space area ratio in downtown of Changchun and Jilin cities during 2000–2019. CNY: Chinese yuan, equivalent to yuan (RMB)

promote regional equality of development by guiding progress in small and medium cities.

The critical issue is the expansion of cities that encroached on cropland, although this trend was waning (Fig. 8f). The issue existed for a long time (He et al., 2017; Qiu et al., 2020), which was linked to economic development in JLC. For example, the reduction in the occupied cropland concurrently with the economic downturn in 2010–2015 (Fig. 6f, Fig. 8a). To prevent the loss of cropland and ensure food production, urban development boundaries need to be established and supervised. In this regard, the National Eco-Functional Zoning Plan and the National New-Type Urbanization Plan have been launched to restrict disorderly urban expansion; the restrictive effects of these policies on urban expansion and the impact on food production need to be observed in the future.

5 Conclusions

The present study considered the evolution of policies and LULC in a typical agriculture-forest ecotone JLC. Five time-slice LULC maps with 15 m resolution were generated to match the time nodes of various policies during 2000–2019. Our observations show that the cropland expansion in JLC was obvious; however, it was accompanied by a decrement of agricultural GDP proportion and a slight increment of grain yield. With the net conversion area of forest to cropland in a decreasing

trend, the deciduous forest area increased. In the key urban agglomeration, with the increment of the urban settlement area, the green space area also increased. The raised green space ratio made for improving the urban thermal environment and carbon balance. Through considering twelve administrative measures shows that policies and projects have driven LULC changes. Agricultural policies strengthened agricultural productivity and promoted the cropland expansion; however, the expansion did not generate substantial profits because of the poor cultivating structure. Thus, the implementation space of the Grain to Green project was compressed, constituted a trade-off relationship between environmental policies and agricultural policies. The economic and urbanization policies guided the economic development, greening, and environmental improvement of key urban agglomerations, forming a harmonious development of humans and land. JLC, as an ecotone integrating agri-food production zone, eco-regulation zone, and key urban agglomerations, demonstrates the complexity of current major administrative measures that aim to promote land use optimization and sustainable development in Northeast China. In the future, decision-makers should focus on optimizing crop planting structure to achieve the synergy of agricultural development and environmental restoration; besides, policies should also ensure the equality of socio-economic development among cities.

Appendix Table

Table S1 Accuracy assessment of land use land cover maps

LULC	Accuracy	Forest	Grassland	Wetland	Water body	Cropland	Impervious	Bareland
Tier-1 type	UA	0.967 ± 0.02	0.705 ± 0.07	0.902 ± 0.06	0.975 ± 0.02	0.923 ± 0.03	0.954 ± 0.02	0.935 ± .04
	PA	0.881 ± 0.02	0.030 ± 0.00	0.968 ± 0.07	0.945 ± 0.02	0.992 ± 0.04	0.887 ± 0.02	0.670 ± 0.03
	OA	0.939 ± 0.02						
LULC	Accuracy	Coniferous forest		Deciduous forest		Rice paddy	Dryland	
Tier-2 type	UA	0.926 ± 0.03		0.875 ± 0.04		0.978 ± 0.02	0.937 ± 0.03	
	PA	0.910 ± 0.03		0.897 ± 0.04		0.910 ± 0.02	0.897 ± 0.03	
	OA	0.889 ± 0.03				0.795 ± 0.03		

Notes: Accuracy is presented with a 95% confidence interval. UA: user's accuracy, PA: producer's accuracy, OA: overall accuracy

References

- Bryan B A, Gao L, Ye Y Q et al., 2018. China's response to a national land-system sustainability emergency. *Nature*, 559(7713): 193–204. doi: 10.1038/s41586-018-0280-2
- CCCCP (Central Committee of the Communist Party of China), 2011. *Outline of Poverty Alleviation and Development in China's Rural Areas (2011–2020)*. Available via DIALOG. http://www.gov.cn/gongbao/content/2011/content_2020905.htm. Cited 7 Jan 2021. (in Chinese)
- CCCCP (Central Committee of the Communist Party of China), 2014. *National New-Type Urbanization Plan (2014–2020)*. Available via DIALOG. http://www.gov.cn/gongbao/content/2014/content_2644805.htm. Cited 7 Jan 2021. (in Chinese)
- Chen H J, Wang G P, Lu X G et al., 2015. Balancing the Needs of China's Wetland Conservation and Rice Production. *Environmental Science & Technology*, 49(11): 6385–6393. doi: 10.1021/es505988z
- CSC (China State Council), 2002. *Regulations on Returning Farmland to Forests*. Available via DIALOG. http://www.gov.cn/gongbao/content/2002/content_61463.htm. Cited 7 Jan 2021. (in Chinese)
- CSC (China State Council), 2009. *Opinions on Further Implementing the Strategy of Revitalizing Northeast China and Other Old Industrial Bases*. Available via DIALOG. http://www.gov.cn/gongbao/content/2009/content_1417927.htm. Cited 7 Jan 2021. (in Chinese)
- Dong J W, Xiao X M, Menarguez M A et al., 2016. Mapping paddy rice planting area in northeastern Asia with Landsat 8 images, phenology-based algorithm and Google Earth Engine. *Remote Sensing of Environment*, 185: 142–154. doi: 10.1016/j.rse.2016.02.016
- Dong Y L, Ren Z B, Fu Y et al., 2020a. Recording urban land dynamic and its effects during 2000–2019 at 15-m resolution by cloud computing with Landsat series. *Remote Sensing*, 12(15): 2451. doi: 10.3390/rs12152451
- Dong Y L, Ren Z B, Wang Z M et al., 2020b. Spatiotemporal patterns of forest changes in Korean peninsula using Landsat images during 1990–2015: a comparative study of two neighboring countries. *IEEE Access*, 8: 73623–73633. doi: 10.1109/access.2020.2988122
- Feddema J J, Oleson K W, Bonan G B et al., 2005. The importance of land-cover change in simulating future climates. *Science*, 310(5754): 1674–1678. doi: 10.1126/science.1118160
- He C Y, Liu Z F, Xu M et al., 2017. Urban expansion brought stress to food security in China: Evidence from decreased cropland net primary productivity. *Science of the Total Environment*, 576: 660–670. doi: 10.1016/j.scitotenv.2016.10.107
- Houghton R A, House J I, Pongratz J et al., 2012. Carbon emissions from land use and land-cover change. *Biogeosciences*, 9(12): 5125–5142. doi: 10.5194/bg-9-5125-2012
- Kuang W H, 2020a. 70 years of urban expansion across China: trajectory, pattern, and national policies. *Science Bulletin*, 65(23): 1970–1974. doi: 10.1016/j.scib.2020.07.005
- Kuang W H, 2020b. National urban land-use/cover change since the beginning of the 21st century and its policy implications in China. *Land Use Policy*, 97: 104747. doi: 10.1016/j.landusepol.2020.104747
- Kuang Wenhui, 2020c. Seasonal variation in air temperature and relative humidity on building areas and in green spaces in Beijing, China. *Chinese Geographical Science*, 30(1): 75–88. doi: 10.1007/s11769-020-1097-0
- Kuang W H, Dou Y Y, 2020. Investigating the patterns and dynamics of urban green space in China's 70 major cities using satellite remote sensing. *Remote Sensing*, 12(12): 1929. doi: 10.3390/rs12121929
- Kuang W H, Yan F Q, 2018. Urban structural evolution over a century in Changchun City, northeast China. *Journal of Geographical Sciences*, 28(12): 1877–1895. doi: 10.1007/s11442-018-1569-7
- Lai L, Huang X J, Yang H et al., 2016. Carbon emissions from land-use change and management in China between 1990 and 2010. *Science Advances*, 2(11): e1601063. doi: 10.1126/sciadv.1601063
- Lammert M, Allan J D, 1999. Assessing biotic integrity of streams: Effects of scale in measuring the influence of land use/cover and habitat structure on fish and macroinvertebrates. *Environmental Management*, 23(2): 257–270. doi: 10.1007/s002679900184
- Liang L, Xu B, Chen Y L et al., 2010. Combining spatial-temporal and phylogenetic analysis approaches for improved understanding on global H5N1 transmission. *PloS One*, 5(10): e13575. doi: 10.1371/journal.pone.0013575
- Liu J G, Li S X, Ouyang Z Y et al., 2008. Ecological and socioeconomic effects of China's policies for ecosystem services. *Proceedings of the National Academy of Sciences of the United States of America*, 105(28): 9477–9482. doi: 10.1073/pnas.0706436105
- Liu T X, Zhang S W, Yu L X et al., 2017. Simulation of regional temperature change effect of land cover change in agroforestry ecotone of Nenjiang river basin in China. *Theoretical and Applied Climatology*, 128: 971–981. doi: 10.1007/s00704-016-1750-9
- Liu Y S, Fang F, Li Y H, 2014. Key issues of land use in China and implications for policy making. *Land Use Policy*, 40: 6–12. doi: 10.1016/j.landusepol.2013.03.013
- Luo L, Mao D H, Wang Z M et al., 2018. Remote sensing and GIS support to identify potential areas for wetland restoration from cropland: a case study in the west Songnen plain, northeast China. *Sustainability*, 10(7): 2375. doi: 10.3390/su10072375
- Mao D H, He X Y, Wang Z M et al., 2019. Diverse policies leading to contrasting impacts on land cover and ecosystem services in Northeast China. *Journal of Cleaner Production*, 240: 117961. doi: 10.1016/j.jclepro.2019.117961
- Mao D H, Luo L, Wang Z M et al., 2018. Conversions between natural wetlands and farmland in China: a multiscale geospa-

- tial analysis. *Science of the Total Environment*, 634: 550–560. doi: 10.1016/j.scitotenv.2018.04.009
- MEE (Ministry of Ecology and Environment), 2015. *Announcement on the Issuance of National Ecological Function Regionalization*. Available via DIALOG. http://www.mee.gov.cn/gkml/hbb/bgg/200910/t20091022_174499.htm. Cited 18 Aug 2020. (in Chinese)
- NDRC (National Development and Reform Commission), 2016. *Three-year Rolling Implementation Plan for Revitalizing Northeast China and Other Old Industrial Bases (2016–2018)*. Available via DIALOG. http://www.gov.cn/xinwen/2016-08/22/content_5101326.htm. Cited 7 Jan 2021. (in Chinese)
- NFGA (National Forestry and Grassland Administration), 2013. *Notice on Effectively Strengthening the Construction of the Fifth Phase of the Three North Shelterbelt Project*. Available via DIALOG. <http://www.forestry.gov.cn/portal/zlszz/s/4249/content-692208.html>. Cited 7 Jan 2021. (in Chinese)
- Olofsson P, Foody G M, Herold M et al., 2014. Good practices for estimating area and assessing accuracy of land change. *Remote Sensing of Environment*, 148: 42–57. doi: 10.1016/j.rse.2014.02.015
- Otsu N, 1979. Threshold selection method from gray-level histograms. *IEEE Transactions on Systems Man and Cybernetics*, 9(1): 62–66. doi: 10.1109/tsmc.1979.4310076
- PHRC (Party History Research Center of the CPC Central Committee), 2009. *Footprints of the People's Republic of China*. Beijing: Xinhua Publishing House. (in Chinese)
- Qiu B W, Li H W, Tang Z H et al., 2020. How cropland losses shaped by unbalanced urbanization process? *Land Use Policy*, 96: 104715. doi: 10.1016/j.landusepol.2020.104715
- Ren Z B, He X Y, Pu R L et al., 2018. The impact of urban forest structure and its spatial location on urban cool island intensity. *Urban Ecosystems*, 21(5): 863–874. doi: 10.1007/s11252-018-0776-4
- Ren Z B, Zheng H F, He X Y et al., 2019. Changes in spatio-temporal patterns of urban forest and its above-ground carbon storage: Implication for urban CO₂ emissions mitigation under China's rapid urban expansion and greening. *Environment International*, 129: 438–450. doi: 10.1016/j.envint.2019.05.010
- Rockstrom J, Steffen W, Noone K et al., 2009. A safe operating space for humanity. *Nature*, 461(7263): 472–475. doi: 10.1038/461472a
- van Donkelaar A, Martin R V, Brauer M et al., 2016. Global estimates of fine particulate matter using a combined geophysical-statistical method with information from satellites, models, and monitors. *Environmental Science & Technology*, 50(7): 3762–3772. doi: 10.1021/acs.est.5b05833
- Wu W H, Chen Z F, Li Y H et al., 2019. Land engineering and its role for sustainable agriculture in the agro-pastoral ecotone: a case study of Yulin, Shaanxi Province, China. *Journal of Geographical Sciences*, 29(5): 818–830. doi: 10.1007/s11442-019-1630-1
- Yang R, Li X Y, Mao D H et al., 2020. Examining fractional vegetation cover dynamics in response to climate from 1982 to 2015 in the Amur river basin for SDG 13. *Sustainability*, 12(14): 5866. doi: 10.3390/su12145866
- Ye Y, Fang X Q, 2012. Expansion of cropland area and formation of the eastern farming-pastoral ecotone in northern China during the twentieth century. *Regional Environmental Change*, 12(4): 923–934. doi: 10.1007/s10113-012-0306-5
- Zhao L J, Zheng K, Shi L L et al., 2019a. Remote sensing image sample dataset of land cover types in China. *China Scientific Data*, 4(2): 196–207. doi: 10.11922/csdata.2018.0058.zh
- Zhao Y Y, Feng D L, Yu L et al., 2019b. Long-term land cover dynamics (1986–2016) of northeast China Derived from a Multi-temporal Landsat Archive. *Remote Sensing*, 11(5): 599. doi: 10.3390/rs11050599